JOURNAL OF CATALYSIS **166,** 356–367 (1997)
ARTICLE NO. CA971499

Selective Reduction of NO by NH_3 over Chromia on Titania Catalyst: Investigation and Modeling of the Kinetic Behavior

R. Willi, M. Maciejewski, U. Göbel, R. A. Köppel, and A. Baiker[1,2]

Department of Chemical Engineering and Industrial Chemistry, Swiss Federal Institute of Technology, ETH-Zentrum, CH-8092 Zurich, Switzerland

Received August 28, 1996; accepted October 8, 1996

The kinetics and the parametric sensitivity of the selective catalytic reduction (SCR) of NO by NH_3 were investigated over a chromia on titania catalyst. The chromium oxide phase was made up predominantly of X-ray amorphous Cr_2O_3. High SCR activity and selectivity to N_2 was attained at low temperatures. The high selectivity is attributed to the absence of significant amounts of CrO_2 and crystalline α-Cr_2O_3 which favor N_2O formation. The selectivity to N_2O increased with higher temperature. Addition of up to 6% H_2O to the dry feed reduced the rate of NO conversion and decreased the undesired formation of N_2O. The effect of water on the catalytic behavior was reversible. In the absence of oxygen, the reaction between NO and NH_3 became marginal, independently whether H_2O was present or not. Small amounts of oxygen were sufficient to restore SCR activity. Admission of SO_2 to the SCR feed resulted in a severe loss of activity. The poisoning of the catalyst by SO_2 was already notable for low SO_2 concentrations (30 ppm) and for temperatures up to 573 K. X-ray photoelectron and FTIR spectroscopy revealed the presence of sulfate species on the catalyst surface. Analysis of the kinetic data indicated that the SCR reaction is first order in NO and zeroth order in NH_3 for temperatures in the range 400–520 K. The estimated activation energies for dry and wet feed amounted to 60.0 ± 1.6 kJ/mol (95% confidence limits). For temperatures in the range 400–520 K, and for a SO_2 free feed, the steady-state kinetic data could be well described with a model based on an Eley–Rideal type reaction between activated ammonia surface species and gaseous or weakly adsorbed NO.

INTRODUCTION

NO_x is a source of photochemical smog and contributes to acid rain. For this reason several countries, above all Japan, the United States, and Germany, established programs for the reduction of the NO_x emissions in the early 1970s. As a consequence, various methods of combustion control and flue gas treatment were developed. The selective catalytic reduction of NO_x with ammonia is the most proven and effective method for the post-combustion control of the NO_x emission (1).

Various materials have been investigated for their application as SCR catalysts. One of the most effective catalysts is vanadia on titania, frequently in combination with tungsten and/or molybdenum oxide. Other oxides have received less attention. Recently, chromia-containing catalysts have been reported to exhibit interesting properties for the reduction of nitric oxide with ammonia in the presence of excess oxygen (2, 3), especially in the low-temperature range. Bulk amorphous chromium oxide was shown to be highly active at low temperatures affording nitrogen with high selectivity, whereas crystalline chromia (α-Cr_2O_3) produces substantial amounts of nitrous oxide and also exhibits significant activity for ammonia oxidation (4, 5). Differences in the catalytic behavior of these unsupported chromia catalysts are correlated with the higher density of labile oxygen species available on the surface of the amorphous sample under SCR reaction conditions (6).

In studies of supported chromium oxide catalysts it has been demonstrated that the behavior in SCR is strongly influenced by the support as well as by the nature of the chromia surface species. Wong *et al.* (7) reported that TiO_2-supported chromia catalysts were generally more active than Al_2O_3-supported catalysts and that formation of undesired N_2O was higher for the titania-supported catalyst. Previous investigations performed in our group with CrO_x/TiO_2 catalysts have shown that the supported chromium species are characterized by pronounced oxidation-reduction chemistry. The nature and oxidation state of the chromium oxide species depends on the Cr loading, preparation procedure, and on the pretreatment conditions (8). It was demonstrated that the various chromium oxide phases, i.e., CrO_2, CrOOH, and Cr_2O_3 differ markedly in their activity and selectivity (9). The highest activity combined with a high selectivity to N_2 was found for X-ray amorphous Cr_2O_3 supported on titania. Crystallization of Cr_2O_3 induced at higher temperatures reduced the activity significantly. Similar high conversion of NO is found with CrO_2/TiO_2, but substantial amounts of undesired N_2O are produced with this catalyst. Supported CrOOH is oxidized to CrO_2 under typical SCR conditions above 570 K and consequently exhibits similar catalytic behavior as CrO_2 (10, 11).

[1] To whom correspondence should be addressed.
[2] Fax: +41-1-632 1163. E-mail: Baiker@tech.chem.ethz.ch.

0021-9517/97 $25.00

A limited number of studies have focused so far on the parametric sensitivity, the mechanism, and the kinetics of the SCR reaction over chromia based catalysts. For vanadia-based catalysts it is well known from the literature that the presence of oxygen in the reaction mixture markedly enhances the activity for the SCR reaction (12–14), whereas water suppresses the reduction of NO (15). Duffy *et al.* (16) investigated the influence of oxygen on the rate and the selectivity of the SCR reaction over amorphous and crystalline chromia. A sharp rise in activity was observed for concentrations up to 1000 ppm O_2 with both forms of chromia. For higher oxygen concentrations the effect leveled off. Willey *et al.* (17) similarly found higher reaction rates in the presence of oxygen for iron oxide–chromia–alumina aerogel catalysts.

Although flue gases usually contain water, most of the laboratory studies of chromia based SCR catalysts have been performed under dry conditions. The effect of water on the reaction of NO and NH_3 over amorphous and crystalline chromia catalysts has been investigated by isotopic labeling experiments by Duffy *et al.* (5). In the presence of excess oxygen, the addition of 1.5% H_2O decreased NO and NH_3 conversions and inhibited the formation of ammonia oxidation products N_2O and NO for temperatures up to 523 K over both forms of chromia. The authors verified that the effect of water on the activity and selectivity was reversible. Köhler *et al.* (8) observed significantly lower activity as well as higher selectivity to N_2O for chromium oxide supported on titania when the SCR feed gas contained water.

Several authors (18, 19) suggested for SCR on supported chromia catalysts a first-order kinetics in nitric oxide and zeroth order in ammonia. Comparable reaction orders in nitric oxide and ammonia were observed for vanadia-based catalysts and several kinetic models were proposed (20–23). However, to our knowledge no model including all relevant exhaust gas components has been reported so far for chromia-based catalysts.

In the present work, a 10 wt% Cr_2O_3/TiO_2 catalyst has been investigated. In order to decrease the amount of CrO_2 and to minimize the formation of α-Cr_2O_3, which both are considered responsible for N_2O formation, the method of catalyst preparation of Maciejewski *et al.* (10) was modified. By directly reducing the dried sample without calcination, predominantly poorly crystalline Cr_2O_3 (>95 wt%) was obtained. Previous studies have concentrated on chemical and structural properties as well as on the catalytic behavior of different chromium oxide phases (CrO_2, CrOOH, Cr_2O_3) in the selective catalytic reduction of NO by NH_3 in excess oxygen. Here we are focusing on the performance and stability of Cr_2O_3/TiO_2 under real SCR conditions, e.g., in the presence of water in the feed. The influence of oxygen, water, and sulfur dioxide on activity and selectivity and on catalyst stability is investigated. The influence of different reaction parameters was studied and a microkinetic model has been developed, which includes the influences of all major exhaust components.

EXPERIMENTAL

Catalyst Preparation

The catalyst was prepared by wet impregnation of TiO_2 (P25, specific surface area 49 m^2/g, supplier Degussa) with chromium(III)nitrate nonahydrate (Fluka) as described in a preceding paper (11). A chromium content of 6.84 wt% Cr, corresponding to 10 wt% Cr_2O_3 was used. After drying at 1×10^4 Pa and 363 K for 2 h and at 413 K for 8 h the catalyst was crushed and sieved to a grain size of 180 to 300 μm. In order to avoid the formation of crystalline CrO_2 upon thermal decomposition of the chromia precursor, the dried catalyst was reduced with pure hydrogen at 523 K for 1 h without precalcination, thus producing mainly CrOOH (11). Heating in argon at 773 K for 5 h resulted in the decomposition of CrOOH to a mixture of poorly crystalline Cr_2O_3 (>95 wt%) besides of a minor amount of undecomposed CrOOH. The BET surface area determined by N_2-physisorption at 77 K using a Micrometrics ASAP 2000 instrument amounted to 49 m^2/g.

Apparatus

Steady-state catalytic studies were carried out in a fully computer controlled apparatus consisting of a gas dosing unit, a continuous tubular fixed-bed microreactor, and an analytical unit. For further details refer to Ref. (24). The flows of all reactant gases were controlled by means of mass flow controllers (Brooks 5850). Water was fed by a step-motor pump and evaporated into the preheated feed stream. The reaction gas mixture consisted of 200–1000 ppm NO (99.0 vol%, PanGas), 200–1000 ppm NH_3 (99.98 vol%, PanGas), 0–6 vol% H_2O (bidistilled), and 0–12 vol% O_2 (99.995 vol%, PanGas) in N_2-balance (99.995 vol% PanGas). The yield of the homogeneous reaction of NO and O_2 to NO_2 was smaller than 3% as evidenced by measurements with an empty reactor. The gas composition at the reactor inlet and outlet was monitored using a quadrupole mass spectrometer (GAM 400 Balzers) and a FTIR-spectrometer (Perkin Elmer System 2000) equipped with a heatable multi-pass gas cell (Infrared Analysis, 100 cc volume, 2.4 m pathlength). Standard experiments were carried out with a feed containing 1000 ppm NO, 1000 ppm NH_3, 10% O_2 in N_2-balance using 0.35 g of catalyst (180–300 μm sieve fraction) and a reactant flow rate of 200–1000 ml (NTP) min^{-1} (60,000–300,000 h^{-1} (NTP) GHSV) at a constant pressure of 1.1 bar in the temperature range 400–520 K.

The selectivities to N_2 and N_2O were calculated according to Eq. [1].

$$S_i = \frac{2 \cdot F_i}{F_{NOin} + F_{NH_3in} - F_{NOout} - F_{NH_3out}}, \qquad [1]$$

where F_i is the molar flow rate of component i and in and out refer to the reactor inlet and outlet, respectively.

Kinetic Modeling

The model parameters were estimated from the experimental data by linear and nonlinear regression analysis. For the nonlinear regression analysis the simulation software "Simusolv" (version 3.0-120, Dow Chemical Co.) was used. As objective function the maximum likelihood function of the NO and N_2O partial pressures was chosen. The fourth-order Runge–Kutta method was used for the numerical integration and the procedure of Nelder–Mead direct search method for maximizing the objective function.

X-Ray Photoelectron Spectroscopy (XPS)

XPS analysis of the catalyst samples was performed in a Leybold–Heraeus LHS 11 MCD instrument using Mg$K\alpha$ radiation (240 W) to excite photoelectrons. The analyzer was operated at 37.8 eV constant pass energy at an energy scale calibrated versus the Au $4f_{7/2}$ signal at 84.0 eV. Under these conditions the full-width at half-maximum (FWHM) of the Ag $3d_{5/2}$ line was 0.9 eV. To compensate for the steady-state charging effects, binding energies have been normalized with respect to the position of the C 1*s* signal, resulting from the adsorbed hydrocarbons.

Transmission FTIR Spectroscopy

The transmission FTIR spectra were recorded on a Perkin Elmer System 2000 spectrometer. Mixtures of 0.5 mg catalyst sample and KBr (Fluka) were finely ground and agglomerated under pressure (15 MPa, 180 s). The transparent wafers were mounted on a special sample holder in an environmental chamber and heated at 473 K in a flow of dried nitrogen for 1 h. Before measurements the sample was cooled to 323 K to avoid a broadening of the absorption bands. Spectra were recorded with a resolution of 4 cm^{-1} in the range of 4000–450 cm^{-1} accumulating 500 scans. Background spectra were recorded under identical conditions with a pure KBr wafer.

RESULTS

Catalytic Behavior

Due to the small catalyst particle size in comparison to the reactor diameter and a quartz wool layer in front of the catalyst bed, plug flow was established over the whole catalyst bed. Theoretical calculations based on the criterion of Weisz and Prater (25) indicated that no mass transfer limitation occurred in the investigated temperature range. The calculated maximum adiabatic temperature increase for 1000 ppm NO in the feed was about 13 K. The measured experimental increase of the gas temperature for full conversion at the highest space velocity amounted to 1.5 K. Due to the negligible increase of the temperature and the small particle size, temperature gradients in the catalyst bed and catalyst particles were negligible.

Stability of the catalyst. The effect of time on stream on the catalytic behavior of chromia/titania in the selective reduction of NO by NH_3 with and without water in the feed is depicted in Fig. 1 for a temperature of 473 K. Starting with a dry feed, NO conversion and the selectivity to N_2O reached steady state within 30 min. Changing to a feed containing 5% water resulted in an immediate sharp drop in NO conversion from 87 to 42%. Simultaneously a pronounced decrease of the undesired formation of N_2O from 1.9 to 0.5% was observed. NO conversion further decreased with time on stream to reach a new steady-state value of 31% after 2 h, while N_2O selectivity remained constant. The results manifest that the formation of N_2O (73% decrease) is slightly more inhibited in the presence of water than the reduction of NO to N_2 (64% decrease). The previous activity and selectivity of the catalyst was reestablished within several minutes if water was removed from the feed. For a catalyst being on stream for 250 h under varying reaction conditions a decrease in catalytic activity, combined with an increase of the formation of N_2O was observed. Note that the same catalyst was used for consecutive measurements at times in the following experiments thus leading to slightly different conversion and selectivity values for similar reaction conditions. The decrease in activity

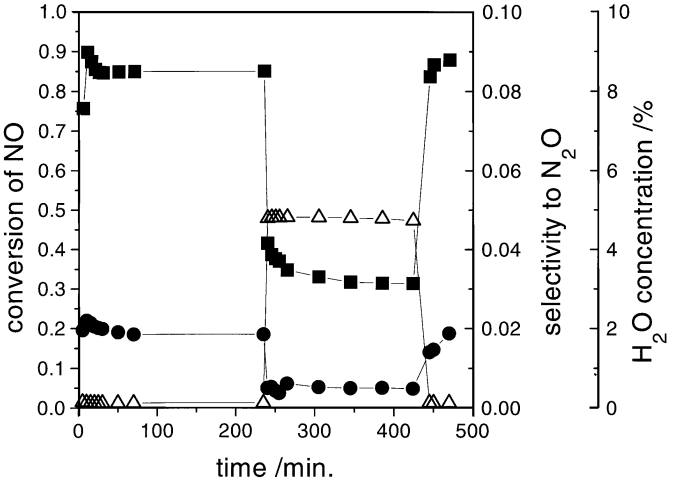

FIG. 1. NO conversion and selectivity to N_2O as a function of time on stream for a chromia/titania catalyst being alternately exposed to dry and wet feed conditions. (■) NO conversion, (●) selectivity to N_2O, (△) H_2O concentration, 0 or 5% H_2O; gas flow rate = 300 ml/min(NTP), $T_{reactor}$ = 473 K.

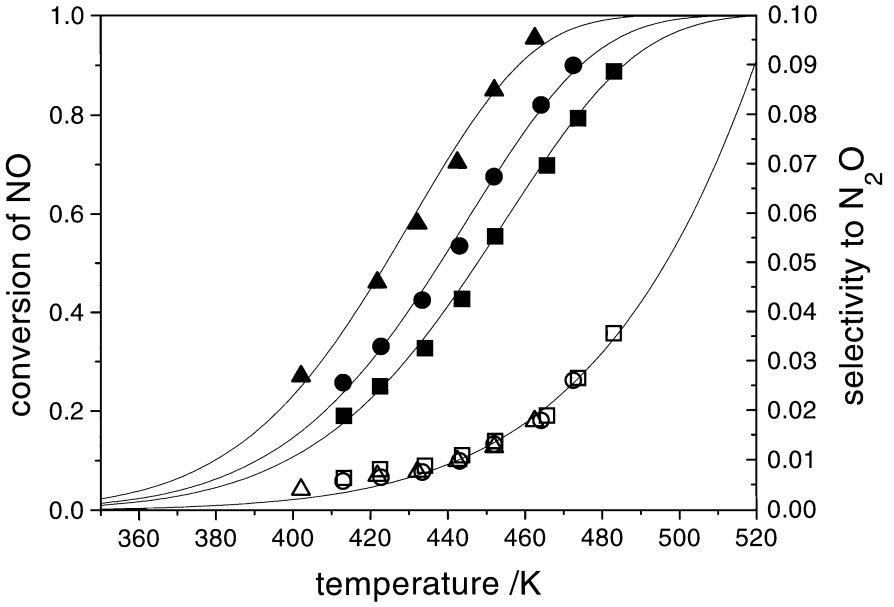

FIG. 2. Conversion of NO (filled symbols) and selectivity to N_2O (open symbols) as a function of temperature for different gas flow rates. (▲, △) 300 ml(NTP)/min, (●, ○) 500 ml(NTP)/min, (■, □) 700 ml(NTP)/min. Symbols indicate measured values, whereas the conversion and selectivity curves (—) were calculated using the model described by Eqs. [4–7] and the preexponential factors $k_1^0 = 1.86E\text{-}2$ m^3/kg s and $k_2^0 = 2.4E\text{-}4$ m^3/kg s.

is thereby reflected by the variation of the corresponding preexponential factors k_1^0 and k_2^0.

Influence of temperature. Figure 2 demonstrates the dependence of the NO conversion and the selectivity to N_2O on the temperature for different gas flow rates. The symbols in this and the subsequent figures indicate measured values, whereas the curves represent the predicted conversions and selectivities from an Eley–Rideal model. A detailed description of the model is presented in a following part of this paper. The temperature dependence of the NO conversion shows that 90% NO are converted at 459 K for a flow rate of 300 ml(NTP)/min (Fig. 2). Increasing the flow rate resulted in an increase of the temperature to obtain 50% NO conversion from 424 K (300 ml/min) to 448 K (700 ml/min). Note that the amounts of NO and NH_3 converted were equal within the experimental error for all experiments (not shown). From Fig. 2 it is also apparent that the selectivity to N_2O is only influenced by the temperature and is independent of the gas flow rate. With raising temperature an increase of the formation of the undesired N_2O is observed.

Influence of gas flow rate. Figure 3 shows the dependence of NO conversion on the ratio catalyst mass to gas flow (W/F) for different temperatures. Increasing the W/F ratio led to higher NO conversions for all temperatures. Integral analysis of the data presented in Fig. 3 revealed reaction orders of one with respect to NO and of zero with respect to NH_3. The reaction orders were confirmed by variation of the inlet concentrations of NO and NH_3 in the range of 200 to 1000 ppm. Good agreement of predicted and measured conversions was achieved over the whole experimental range with the model based on an Eley–Rideal mechanism.

Effect of water. As revealed by Fig. 1, the addition of water substantially influenced the conversion of NO. Figure 4A depicts the decrease in activity caused by water concentrations of 1–6 vol% for temperatures in the range

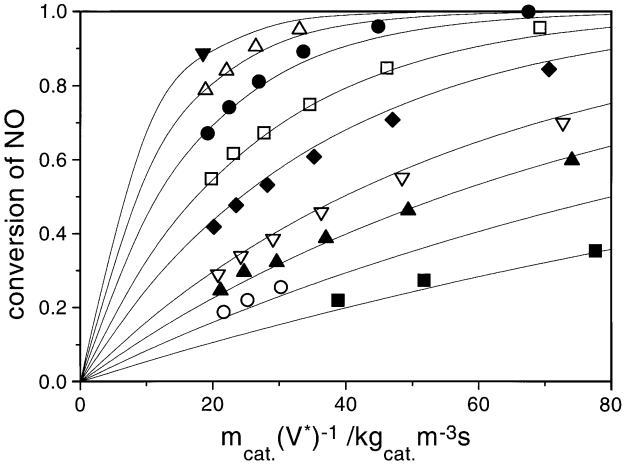

FIG. 3. Influence of the catalyst weight/flow ratio (W/F) on the NO conversion for different temperatures. (■) 402 K, (○) 413 K, (▲) 422 K, (▽) 430 K, (◆) 443 K, (□) 452 K, (●) 463 K, (△) 473 K, (▼) 483 K; catalyst weight = 0.35 g, gas flow rates = 200 ml/min–800 ml(NTP)/min. Symbols indicate measured values, whereas the conversion and selectivity curves (—) were calculated using the model described by Eqs. [4–7] and the preexponential factors $k_1^0 = 1.86E\text{-}2$ m^3/kg s and $k_2^0 = 2.4E\text{-}4$ m^3/kg s.

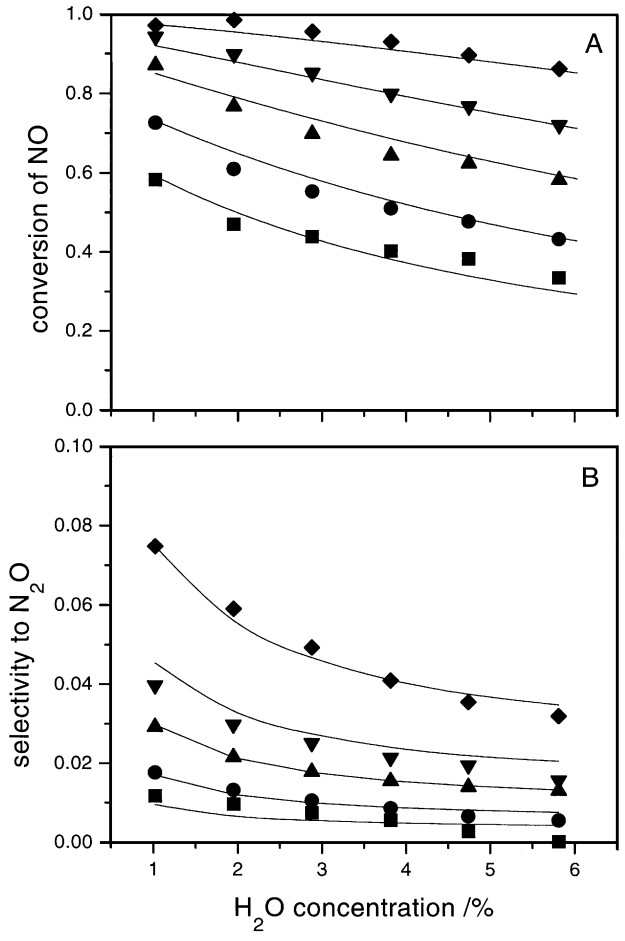

FIG. 4. NO conversion (A) and selectivity to N_2O (B) as a function of the water concentration in the feed gas for different temperatures. (■) 471 K, (●) 481 K, (▲) 492 K, (▼) 500 K, (◆) 512 K; gas flow rate = 500 ml(NTP)/min. Symbols indicate measured values, whereas the conversion and selectivity curves (—) were calculated using the model described by Eqs. [4–7] and the preexponential factors $k_1^0 = 1.2E\text{-}2$ m^3/kg s and $k_2^0 = 3.5E\text{-}4$ m^3/kg s.

471 to 512 K. The effect of water on NO conversion is stronger for low temperatures and low concentrations of H_2O. The experimental data presented in Fig. 4B show that water has not only an impact on the conversion of NO, but also influences substantially the selectivity to nitrous oxide. Addition of water in the range 1–6 vol% strongly suppressed the undesired formation of N_2O, with the effect being more pronounced at higher temperatures where comparably high selectivities to N_2O would be attained in the absence of water. The deviation of measured values from the model predictions is in the range of the experimental error for both NO conversion and N_2O selectivity.

Influence of oxygen concentration. The effect of oxygen on the catalytic behavior is presented in Figs. 5 and 6. In the absence of oxygen, conversion of NO was negligible in the temperature range investigated, irrespective whether dry

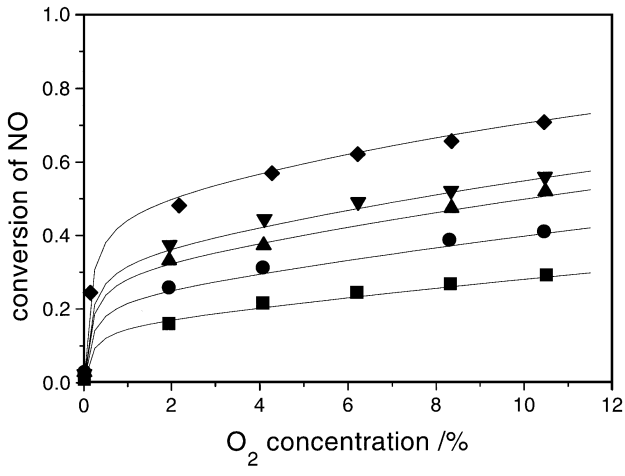

FIG. 5. Influence of oxygen concentration in the feed gas on the NO conversion for a dry feed. (■) 420 K, (●) 431 K, (▲) 440 K, (▼) 444 K, (◆) 456 K; gas flow rate = 500 ml(NTP)/min. Symbols indicate measured values, whereas the conversion and selectivity curves (—) were calculated using the model described by Eqs. [4–7] and the preexponential factors $k_1^0 = 1.76E\text{-}2$ m^3/kg s and $k_2^0 = 5.8E\text{-}4$ m^3/kg s.

or wet conditions were applied. Addition of a low amount of oxygen (1500 ppm) to a dry feed already substantially increased NO conversion, as revealed by the measurements at 456 K (Fig. 5). The increase in NO conversion was most pronounced for oxygen concentrations up to 2 vol% for all temperatures, whereas for concentrations exceeding 2 vol% O_2 the catalyst exhibited an almost linear raise in activity. No significant dependence of the selectivity to N_2O on the oxygen concentration was found.

In the presence of 5 vol% water in the feed gas a similar behavior was observed (Fig. 6), although a linear

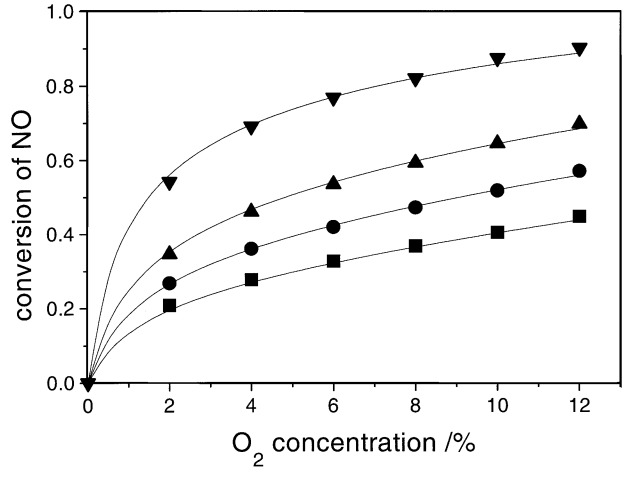

FIG. 6. Influence of oxygen concentration in the feed gas on the NO conversion for a feed containing 5% H_2O. (■) 489 K, (●) 497 K, (▲) 505 K, (▼) 520 K; gas flow rate = 500 ml(NTP)/min. Symbols indicate measured values, whereas the conversion and selectivity curves (—) were calculated using the model described by Eqs. [4–7] and the preexponential factors $k_1^0 = 0.7E\text{-}2$ m^3/kg s and $k_2^0 = 7.5E\text{-}4$ m^3/kg s.

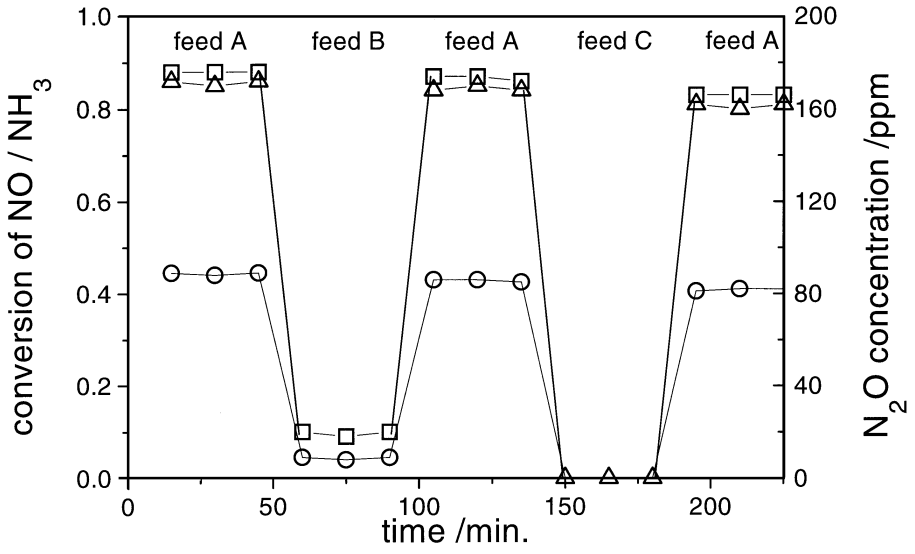

FIG. 7. Influence of feed gas composition on the formation of N_2O and on conversion of NO and NH_3, respectively. (□) NH_3 conversion, (△) NO conversion, (○) N_2O concentration; (feed A): 1000 ppm NO, 1000 ppm NH_3, 10% O_2, 5% H_2O, balance N_2; (feed B): 1000 ppm NH_3, 10% O_2, 5% H_2O, balance N_2; (feed C): 1000 ppm NO, 10% O_2, 5% H_2O, balance N_2, gas flow rate = 500 ml(NTP)/min, $T_{reactor}$ = 505 K.

dependence of NO conversion on oxygen concentration was only found for higher O_2 levels. Similar slopes of the linear raise were observed for oxygen concentrations higher than 6% with both dry and wet feeds.

Influence of the feed gas composition. The dependence of the formation of N_2O on varying the feed gas composition is illustrated in Fig. 7 together with the corresponding conversions of NO and NH_3. Feed A had a composition of 1000 ppm NO, 1000 ppm NH_3, 10% O_2, and 5% H_2O. Feed B contained no nitric oxide, and feed C no ammonia, respectively. Starting with feed A the conversions of NO and NH_3 were comparable within the experimental error. After switching off NO (feed B), the conversion of NH_3 dropped from 86 to 10% and the N_2O concentration decreased simultaneously from 88 to 10 ppm, corresponding to a constant selectivity to N_2O of 10%. The finding shows that the direct oxidation of ammonia by oxygen is comparably small at 505 K and moreover results in a similar selectivity to N_2O. In the absence of ammonia in the feed gas (feed C) NO conversion decreased to zero and the formation of N_2O was completely inhibited. Presented results obtained with feed A and feed B demonstrate that nitrogen and nitrous oxide are predominantly produced by the reaction of NH_3 with NO at 505 K and that the contribution by direct oxidation of ammonia is negligible.

Effect of SO_2. The activity of the catalyst was irreversibly affected by the presence of sulfur dioxide in the feed gas even at low concentrations of SO_2. The poisoning effect of sulfur dioxide as a function of the SO_2 concentration is illustrated in Fig. 8. At a temperature of 503 K 30 ppm of SO_2 in the feed gas are sufficient for a distinct decrease of the NO conversion. The degree of deactivation is a function of the SO_2 concentration and exposure time. During the deactivation SO_2 is completely consumed. After changing to a feed without SO_2 the activity remained stable. Increasing the SO_2 concentration in steps to 60 ppm and further to 90 ppm led to a continuous decrease in NO conversion, while switching off SO_2 resulted in stable activities. No SO_3 was detected in the product stream over the whole experimental period. Running the catalyst at 503 K using the same feed stream without SO_2 for 3 h revealed no change in catalytic activity and the conversion remained on the low level. Attempts were made to regenerate the catalyst by heating at 573 K in a stream of pure nitrogen for 3 h. During this treatment compounds such as ammonium sulfates or ammonium bisulfates formed in the lower temperature range should decompose. However, neither SO_2 nor SO_3 were detected in the effluent gas stream and a subsequent conversion measurement at 503 K showed no increase in activity. If SO_2 was added at 573 K a further deactivation was observed. This indicated that the formation of ammonium sulfates or ammonium bisulfates cannot exclusively explain for the poisoning effect. Moreover, no loss of specific surface area and no significant change in porosity occurred during the SO_2 poisoning experiments. Additional catalytic tests with the partly poisoned catalyst in the temperature range 523 to 573 K showed that not only the reduction of NO to N_2 but also the undesired formation of N_2O was affected by the poisoning. At 573 K and a gas composition of 10% O_2, 1000 ppm NO and 1000 ppm NH_3 in N_2 balance 100% conversion and a selectivity of 98% to N_2 were obtained. Based on the assumption of different sites being responsible for the formation of N_2 and

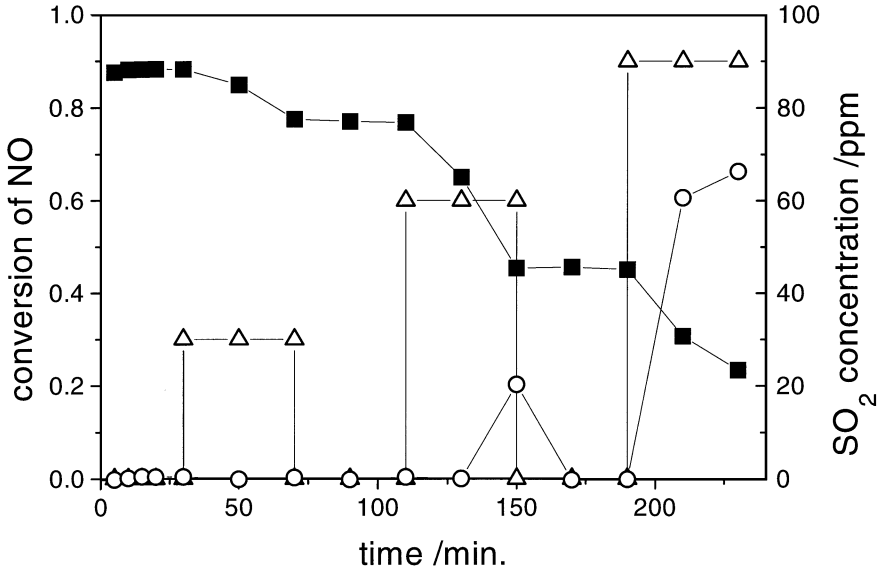

FIG. 8. Effect of SO_2 on the conversion of NO. (△) SO_2 inlet concentration, (○) SO_2 outlet concentration, (■) NO conversion; feed composition: 1000 ppm NO, 1000 ppm NH_3, 10% O_2, 5% H_2O, 0–90 ppm SO_2, balance N_2, gas flow rate = 300 ml(NTP)/min, $T_{reactor}$ = 503 K.

N_2O, we presume that the sites which are involved in the undesired formation of nitrous oxide are much stronger affected by SO_2 than sites which catalyze the reduction of NO to N_2.

XPS Analysis

In order to elucidate the nature of SO_2 poisoning, XPS measurements were made either with fresh catalyst samples or with catalysts exposed to SCR conditions with and without SO_2 in the feed. Part of the samples were washed three times with bidistilled water at a temperature of 353 K for 8 h and subsequently dried under vacuum at 400 K. XPS measurements were made with the washed and unwashed samples. Figure 9 shows the sulfur 2*p* signal which was only observed for the samples exposed to feeds containing SO_2. The binding energy of 169.1 eV indicates that sulfur is present as a sulfate species (26, 27), but whether it is an adsorbed species or part of an ammonium or chromium complex is not clear. Dickinson *et al.* (28) reported a sulfur 2*p* binding energy of 169.1 eV with an asymmetric component on the higher binding energy side for chromium sulfate. The binding energy of the S 2*p* orbital of $(NH_4)_2SO_4$ is found at 168.3 eV (29), which is substantially lower than the value observed in the present work. Moreover, no significant changes in the signals for the other elements (O 1*s*, Cr 2*p*, C 1*s*), and especially of the N 1*s* signal, were observed. In addition, the signal due to sulfur is still present after treatment of the catalyst with water (Fig. 9B), which should eliminate soluble ammonium sulfate. This suggests that predominantly a sulfate type complex of chromium (or titanium) is present on the catalyst surface. Upon treatment of the catalyst with water at 353 K, the semiquantitative analysis revealed a decrease of the sulfur surface concentration from 1.6 to 1.2 at.% and a concomitant increase of the chromium surface concentration from 7.7 to 9.3 at.%, thus indicating that the detected sulfate species could partly originate from soluble ammonium sulfates or ammonium bisulfates.

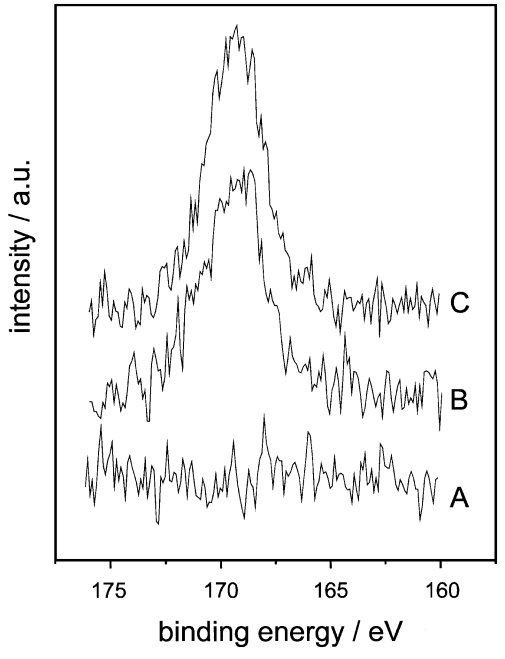

FIG. 9. XP spectra of S 2*p* core level of (A) fresh catalyst, (C) catalyst after SCR reaction in a feed containing 90 ppm SO_2, and (B) the same catalyst after subsequent treatment with water at 353 K for 8 h to remove soluble sulfate species.

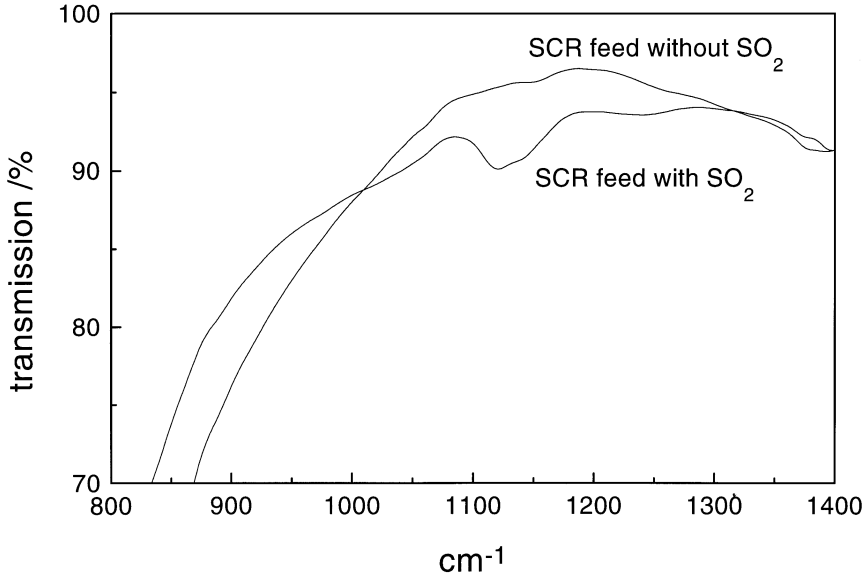

FIG. 10. Transmission FTIR-spectra of a catalyst after SCR reaction with a SO_2 free feed and with a feed containing 90 ppm SO_2, respectively.

Transmission FTIR-Spectroscopy

The transmission FTIR measurements were made with catalyst samples after use in SCR with and without SO_2 in the feed. Only one weak additional band at 1115 cm^{-1} was perceptible (Fig. 10) upon exposure of the catalyst to a feed containing 90 ppm SO_2. No other significant differences in the spectra were observed. The reported ranges of the characteristic absorptions of sulfates (1000–1420 cm^{-1}) and sulfites (980–1225 cm^{-1}) (30) include the observed band. This is a further indication that a sulfate or sulfite type species was formed on the catalyst surface during the exposure to the SO_2 containing SCR-feed.

Kinetic Modeling

The kinetic model used to describe the experimental results was based on the overall stoichiometric reactions expressed by the Eqs. [2] and [3]. Equation [2] represents the main reaction of the selective catalytic reduction of NO for an oxygen containing flue gas, whereas Eq. [3] describes the side reaction responsible for the undesired formation of nitrous oxide. In all experiments the amounts of NO and NH_3 consumed during the reaction were comparable within the experimental error, indicating that NO reacts stoichiometrically with NH_3 under the reaction conditions investigated. Regarding the stoichiometry of the side reaction, the experimental results depicted in Fig. 7 suggest that in the presence of water N_2O is predominantly formed by the stoichiometric reaction of NO with NH_3 in the investigated temperature range. However, substantial amounts of ammonia are oxidized directly to N_2 and N_2O in the absence of NO (Fig. 7). These findings support the assumption of a reaction stoichiometry according to Eqs. [2] and [3] under typical SCR conditions over Cr_2O_3/TiO_2.

$$4\,NO + 4\,NH_3 + O_2 \rightarrow 4\,N_2 + 6\,H_2O \qquad [2]$$

$$4\,NO + 4\,NH_3 + 3\,O_2 \rightarrow 4\,N_2O + 6\,H_2O \qquad [3]$$

Different approaches based on Langmuir–Hinselwood and Eley–Rideal models were investigated for setting up the kinetic equations. The number of kinetic parameters was minimized in order to prevent an overfitting of the obtained results. The best description of the kinetics was achieved with the following approach:

The reaction rate is first order in NO and zeroth order in ammonia for the main and the side reaction.
The inhibition of the main and side reaction by water is caused by a Langmuir adsorption of water on the active sites.
The reoxidation of the catalyst determines the number of the active sites and can occur with adsorbed oxygen as well as with oxygen from the gas phase.
Water inhibits the reoxidation by a competitive Langmuir type adsorption.

The reaction orders of NH_3 and NO were established by varying the inlet concentrations of NO and NH_3 in the range of 200 to 1000 ppm and by integral analysis, which involves a comparison of the experimental datal with values predicted by the model. The zeroth order in ammonia suggests a strong adsorption of ammonia. The assumption that the main and the side reaction have the same reaction orders implies that a variation of the NO or NH_3 concentration has no effect on selectivity. Figure 2 indeed shows that the same selectivity is observed for different conversions

upon varying the gas flow rate at a constant temperature. As different conversions involve different concentrations of NO and NH_3, this finding confirms our assumption.

The inhibition by water could be caused by the competitive adsorption of water and ammonia, but no sufficient fitting was achieved under this assumption. Good fitting was obtained on condition that part of the active sites are covered independently by water. The temperature dependencies of the adsorption equilibrium constants $K_{H_2O_{(1)}}$ and $K_{H_2O_{(2)}}$ were significant which allowed us to estimate the heats of adsorption (ΔH_{H_2O}) and the preexponential factors ($K^0_{H_2O}$) for the main and the side reaction (Table 1).

For the reoxidation of the catalyst gaseous as well as adsorbed oxygen were taken into account. This can be justified by the observed sharp increase of NO conversion in the range of low oxygen concentrations and the linear dependence in the higher O_2 concentration range. Worse fitting was obtained if only one type of reoxidation was considered. An empirical weighing factor was introduced to account for the different influence on reoxidation by either gaseous or adsorbed oxygen. The promoting effect of oxygen has to be the same for the main and the side reaction because the selectivity was independent of the oxygen concentration. The observed inhibiting effect of water on the adsorption of oxygen was considered in the model by taking into account competitive adsorption of O_2 and H_2O.

In order to prevent any distortion of the parameter estimation by the observed slow decrease of catalytic activity and the simultaneous slight increase of the selectivity to N_2O with time on stream, the preexponential factors were adjusted according to the aging of the catalyst. Separate parameter estimation with used and fresh catalysts showed that only the preexponential factors $k^0_1(T_{ref.})$ and $k^0_2(T_{ref.})$ changed. Based on this assumption the reaction rates for the reduction to N_2 (r_1) and for the formation of N_2O (r_2), respectively, are described by the equations

$$r_1 = k_1\left(np_{O_2} + \frac{K_{O_2}p_{O_2}}{1 + K_{O_2}p_{O_2} + K_W p_{H_2O}}\right) \times \frac{1}{1 + K_{H_2O_{(1)}}p_{H_2O}}p_{NO} \quad [4]$$

$$r_2 = k_2\left(np_{O_2} + \frac{K_{O_2}p_{O_2}}{1 + K_{O_2}p_{O_2} + K_W p_{H_2O}}\right) \times \frac{1}{1 + K_{H_2O_{(2)}}p_{H_2O}}p_{NO} \quad [5]$$

$$k_i(T) = k^0_i(T_{ref.})\exp\left(\frac{-E_{A_i}}{R}\left(\frac{1}{T} - \frac{1}{T_{ref.}}\right)\right) \quad [6]$$

$$K_{H_2O_{(i)}}(T) = K^0_{H_2O_{(i)}}(T_{ref.}) \times \exp\left(\frac{-\Delta H_{H_2O_{(i)}}}{R}\left(\frac{1}{T} - \frac{1}{T_{ref.}}\right)\right) \quad [7]$$

$$T_{ref.} = 450\ \text{K}.$$

To reduce the correlation between the preexponential factors ($k^0_i(T_{ref.})$, $K^0_{H_2O}(T_{ref.})$), the activation energies (E_{A_i}), and the enthalpies of adsorption (ΔH_i), the reaction rate constants (k_i) and the equilibrium constant of adsorption ($K_{H_2O_{(i)}}$) were expressed as proposed by Himmelblau (31). All estimated parameters of the kinetic model are listed in Table 1.

TABLE 1

Estimated Parameters for Kinetic Model Described by Eqs. [4–7]

Parameter	Value	Standard deviations	Units
k^0_1	1.9*E*-2–0.7*E*-2	0.01*E*-2–0.06*E*-2	m^3/kg s
E_{A_1}	60	0.8	kJ/mol
k^0_2	2.4*E*-4–7.5*E*-4	0.04*E*-4–0.6*E*-4	m^3/kg s
E_{A_2}	115	1.6	kJ/mol
$K^0_{H_2O_{(1)}}$	6.0*E*-4	0.7*E*-4	Pa^{-1}
$\Delta H_{H_2O_{(1)}}$	−43	4	kJ/mol
$K^0_{H_2O_{(2)}}$	1.5*E*-2	0.3*E*-2	Pa^{-1}
$\Delta H_{H_2O_{(2)}}$	−77	4	kJ/mol
n	8.9*E*-5	0.7*E*-5	Pa^{-1}
K_{O_2}	4.8*E*-3	0.6*E*-3	Pa^{-1}
K_w	1.2*E*-3	0.3	Pa^{-1}

DISCUSSION

The kinetic behavior of the 10 wt% Cr_2O_3/TiO_2 catalyst is comparable with findings of Wong and Nobe (19) for titania-supported vanadia and chromia catalysts for which a reaction rate first order in NO and zeroth order in NH_3 is proposed. The integral analysis of the experimental data revealed a zeroth order reaction with respect to NH_3, suggesting that the catalyst is completely covered by ammonia under reaction conditions, which is reasonable for low temperatures. At higher temperatures and for low ammonia concentrations the coverage is not complete and ammonia adsorption has to be considered in the model (32). Based on temperature-programmed desorption and *in situ* diffuse reflectance FTIR measurements, Schneider *et al.* (33) proposed that the presence of Brønsted bound ammonia is a necessary requirement for the reduction of NO to N_2 over CrO_x/TiO_2.

The observed first-order reaction with respect to NO indicates that gaseous NO is involved in the rate-limiting step. This finding would support and Eley–Rideal mechanism, as proposed similarly for vanadia-based catalysts. The same reaction order in NO would be expected if the adsorption

of NO is involved in the rate-limiting step. As opposed to vanadia-based catalysts, where the adsorption of NO has only been reported under reducing conditions (34, 35), the adsorption of NO on chromia was observed by several authors. Kugler *et al.* (36) suggested that nitric oxide adsorbs on reduced chromia surface in the form of a *cis*-N_2O_2 dimer and as an NO_2 chelate surface complex. The same surface species were observed on α-Cr_2O_3 but not on amorphous chromia (37). On α-Cr_2O_3, these two species are discussed to be formed by oxidation of adsorbed NH_3 molecules and are intermediates on the reaction pathway to N_2O (37). Schneider *et al.* (9) observed by FTIR bands due to surface bound NO under reaction conditions on CrO_2/TiO_2, but not on Cr_2O_3/TiO_2. The question whether adsorbed or gaseous NO reacts with ammonia on the surface of chromium-based catalysts is still unresolved and no conclusive statement can be given based on experimental evidence.

In analogy with supported vanadia catalysts, Schneider *et al.* (9) observed Brønsted sites even at higher temperatures for Cr_2O_3/TiO_2 catalysts. During SCR, N_2O is formed by oxidation of Lewis-bound ammonia with NO and/or oxygen present in the feed gas. In the case of Cr_2O_3, with no adsorbed NO, oxidation of ammonia to N_2O occurs at temperatures higher than 450 K (9). In the absence of NO only Lewis bound ammonia is observed above 420 K, which is oxidized to N_2 and N_2O (33). At higher temperatures ammonia oxidation to NO is favored in the presence of oxygen. In our experiments we observed in the presence of NO that N_2O was mainly formed by the reaction of NH_3 with NO (Fig. 7). The direct oxidation of NH_3 by O_2 to N_2, N_2O and H_2O was negligible in comparison to the main reaction. However, based on our results it cannot be excluded that NH_3 is oxidized to NO in a first step, followed by subsequent reaction to N_2 and N_2O under certain conditions. The fact that differences in the selectivity of used and fresh catalysts have only an influence on the preexponential factors indicates that the reaction to N_2 and N_2O, respectively, occur on different sites in accordance with findings by Schneider *et al.* (9, 33). The estimated adsorption enthalpy of water amounted to -43 kJ/mol for the reaction to N_2, and -77 kJ/mol for the reaction to N_2O, respectively, which is a further indication of different sites being responsible for the main and the side reaction. Taking into account the estimated adsorption enthalpies and the observed inhibition of the NO conversion, it can be assumed that water adsorbs stronger on a Lewis site than on a Brønsted site.

The role of water in the reversible inhibition of the SCR reaction is not fully understood yet. Water can be involved in the rate-limiting step or block the active sites. If the inhibition by water is due to a competitive adsorption between water and ammonia, the reaction order of ammonia should not equal zero in the presence of water. In the model we assumed kinetics of first order in NO and zeroth order in NH_3 in the presence and absence of water. These assumptions necessitate a linear temperature dependency of the reaction rate in the Arrhenius-type plot. The data depicted in Fig. 11 confirm our assumption of the reaction orders for NO and NH_3 in presence and absence of water in the feed gas.

The variation of ammonia concentration in the feed gas led to small changes of the NO conversion, which were in the range of the experimental error and could also be caused by the observed slow deactivation of the catalyst in

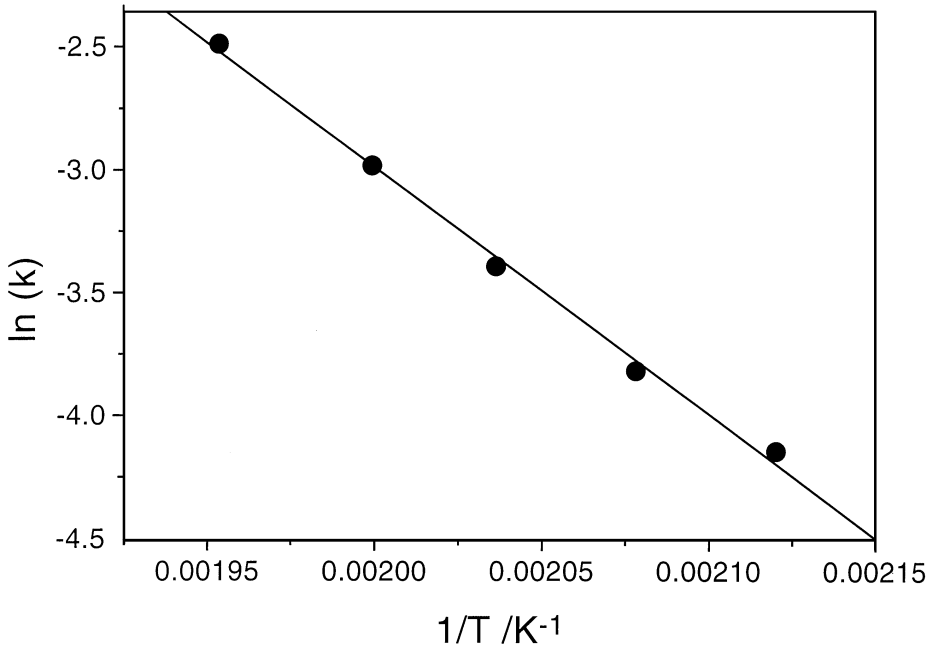

FIG. 11. Arrhenius-type plot for kinetic tests under standard conditions with a feed containing 5% H_2O; gas flow rate = 500 ml(NTP)/min.

the presence of water at higher temperatures. An estimation of the adsorption constant of ammonia in a statistically significant way was not possible due to the lack of accurate data at low NH_3 concentrations. No successful fitting was achieved with models based on an assumption of a competitive adsorption between water and ammonia.

Oxygen plays a crucial role in SCR for vanadia- and chromia-based catalysts (38, 16). Schneider *et al.* (33) demonstrated by TPD experiments that CrO_x/TiO_2 reduced by ammonia is inactive for the selective catalytic reduction of NO. They suggested that a partially oxidized state of the surface must be maintained for SCR. A marked increase in activity and a concomitant decrease in the selectivity to N_2O upon addition of 0.1% O_2 to the SCR feed was also reported for amorphous chromia by Duffy *et al.* (16). In accordance with these results we found that in the absence of oxygen the reaction rate collapsed. Below 1 vol% oxygen in the dry feed, and below 2 vol% oxygen for a feed containing 5 vol% water, a sharp raise in activity was observed with increasing oxygen concentration. For higher oxygen concentrations, a smaller linear increase was found (Figs. 5 and 6). The description of the kinetic conversion curves by a power law approach, implementing a Freundlich isotherm, was not satisfactory. By using a Temkin isotherm good fitting was only achieved for the range between 2 and 10 vol% oxygen and by assuming a pure Langmuir isotherm, only the concentration range below 5 vol% could be fitted properly. The linear dependence of NO conversion on oxygen concentration led us to the assumption that an additional path of reoxidation of the catalyst takes place, which involves gas-phase oxygen and which is significant for higher-oxygen partial pressures. This assumption in combination with the model based on a Langmuir-type adsorption resulted in the best description of the oxygen dependency for the investigated experimental range. Water in the feed gas inhibited the path of the reoxidation via adsorbed oxygen. The inhibition was significant and was taken into account by a competitive adsorption of oxygen and water. The adsorption equilibrium constant was about four times smaller for water than for oxygen.

The nature of SO_2 poisoning of the chromia on titania catalyst differs from fouling effects caused by ammonium sulfate deposition observed on vanadia-based catalysts, where the effect is reversible (39). Ammonium sulfate or bisulfate decomposes at higher temperatures and no fouling is expected for reaction temperatures above 530 K. In our case the catalyst was also poisoned at temperatures of 573 K, as well as in the presence of low SO_2 concentrations. Attempts to reactivate the catalyst either by heating in pure nitrogen at 573 K, or by washing with water failed. Note that no significant change of the specific surface area and the pore size distribution was perceptible after the SO_2 poisoning experiments. Observed changes of the selectivity after the exposure to SO_2 indicate that the process of poisoning may be different for the sites responsible for N_2 and N_2O formation, respectively. The sites which produce N_2O are mainly poisoned by SO_2. XPS as well as FTIR measurements revealed the presence of sulfate species on the catalyst surface. The affinity of these species to the Lewis acid sites seems to be stronger than to the Brønsted sites. This is in accordance with the stronger inhibition by water and the postulated stronger adsorption of ammonia on Lewis acid sites (35). Lower SCR activity upon deposition of sulfate ions on amorphous chromia was attributed by Zhang *et al.* (40) to strong adsorption of NH_3 which prevents chromia from reacting with NO.

CONCLUSIONS

Chromia supported on titania exhibits high activity and selectivity to N_2 in the catalytic reduction of NO in the temperature range 400–520 K. Applying a modified preparation procedure resulted in a catalyst containing >95 wt% poorly crystalline Cr_2O_3, which shows significantly lower tendency for N_2O formation compared to CrO_2 or crystalline α-Cr_2O_3.

The addition of water decreases NH_3 and NO conversion and increases the selectivity to N_2. The effect of water on activity and selectivity is reversible. Similar as with vanadia-based catalysts, the activity collapsed in the absence of O_2 in the feed gas. Low amounts of oxygen resulted in a sharp increase of the reaction rate. The addition of SO_2 led to irreversible poisoning of the catalyst, which restricts application of this catalyst to SO_2 free waste gases.

With a model based on an Eley–Rideal mechanism good prediction of the kinetic behavior was obtained for the temperature range 400–520 K and for a SO_2 free feed gas.

APPENDIX: NOTATION

$m_{\text{cat.}}$	catalyst mass, kg
V^*	gas flow (NTP), m^3/s
r_i	reaction rate, Pa m^3/kg s
k_i	reaction rate constant, m^3/kg s
K_A	adsorption equilibrium constant of component A, Pa^{-1}
k_i^0	pre-exponential factor of the reaction rate constant, m^3/kg s
$K^0_{H_2O_{(i)}}$	pre-exponential factor of the adsorption equilibrium constant of water, Pa^{-1}
$\Delta H_{H_2O_{(i)}}$	adsorption enthalpie of water, kJ/mol
n	empirical weighting factor for the reoxidation

ACKNOWLEDGMENTS

Financial support of this work by the Nationaler Energie-Forschungsfond (NEFF-Project 569) is gratefully acknowledged. The authors thank H. Schneider and K. Köhler for their helpful support in the preparation of the catalyst samples.

REFERENCES

1. Bosch, H., and Janssen, F., *Catal. Today* **2**, 369 (1988).
2. Curry-Hyde, E., and Baiker, A., *Ind. Eng. Chem. Res.* **29**, 1985 (1990).
3. Engweiler, J., Nickl, J., Baiker, A., Köhler, K., Schläpfer, C. W., and von Zelewsky, A., *J. Catal.* **145**, 141 (1994).
4. Curry-Hyde, H. E., Musch, H., and Baiker, A., *Appl. Catal.* **65**, 211 (1990).
5. Duffy, B. L., Curry-Hyde, H. E., Cant, N. W., and Nelson, P. F., *J. Catal.* **154**, 107 (1995).
6. Schraml-Marth, M., Wokaun, A., Curry-Hyde, H. E., and Baiker, A., *J. Catal.* **133**, 415 (1992).
7. Wong, W. C., and Nobe, K., *Ind. Eng. Chem. Prod. Res. Dev.* **25**, 179 (1986).
8. Köhler, K., Engweiler, J., Viebrock, H., and Baiker, A., *Langmuir* **11**, 3423 (1995).
9. Schneider, H., Maciejewski, M., Köhler, K., Wokaun, A., and Baiker, A., *J. Catal.* **157**, 312 (1995).
10. Maciejewski, M., Köhler, K., Schneider, H., and Baiker, A., *J. Solid State Chem.* **119**, 13 (1995).
11. Köhler, K., Maciejewski, M., Schneider, H., and Baiker, A., *J. Catal.* **157**, 301 (1995).
12. Bauerle, G. L., Wu, S. C., and Nobe, K., *Ind. Eng. Chem. Prod. Res. Dev.* **17**, 117 (1978).
13. Inomata, M., Miyamoto, A., and Murakami, Y., *J. Catal.* **62**, 140 (1980).
14. Jung, J., and Panagiotidis, T., *Chemie im Kraftwerk 1990*, 1 (1990).
15. Odenbrand, C. U. I., Gabrielsson, P. L. T., Brandin, J. G. M., and Andersson, L. A. H., *Appl. Catal.* **78**, 109 (1991).
16. Duffy, B. L., Curry-Hyde, H. E., Cant, N. W., and Nelson, P. F., *Appl. Catal. B: Environmental* **5**, 133 (1994).
17. Willey, R. J., Lai, H., and Peri, J. B., *J. Catal.* **130**, 319 (1991).
18. Niiyama, H., Murata, K., and Echigoya, E., *J. Catal.* **48**, 201 (1977).
19. Wong, W. C., and Nobe, K., *Ind. Eng. Chem. Prod. Res. Dev.* **25**, 179 (1986).
20. Nam, I. S., Eldridge, J. W., and Kittrell, J. R., *Ind. Eng. Chem. Prod. Res. Dev.* **25**, 186 (1986).
21. Robinson, W. R. A. M., van Ommen, J. G., Woldhuis, A., and Ross, J. R. H., "Proceedings, 10th International Congress on Catalysis, Budapest, 1992" (L. Guzí *et al.*, Eds.), p. 2673. Akadémiai Kaidó, Budapest, 1993.
22. Tufano, V., and Turco, M., *Appl. Catal. B: Environmental* **2**, 133 (1993).
23. Dumesic, J. A., Topsøe, N.-Y., Slabiak, T., Morsing, P., Clausen, B. S., Törnqvist, E., and Topsøe, H., "Proceedings, 10 International Congress on Catalysis, Budapest, 1992" (L. Guzi *et al.*, Eds.), p. 1325. Akadémiai Kaidó, Budapest, 1993.
24. Willi R., Köppel R. A., and Baiker, A., *Ind. Eng. Chem. Res., in press.*
25. Weisz, P. B., and Prater, C. D., *Adv. Catal. Rel. Subj.* **6**, 144 (1954).
26. Briggs, D., and Seah, M. P., "Practical Surface Analysis by Auger and X-Ray Photoelectron Spectroscopy," Wiley, Chichester, 1985.
27. Wagner, C. D., *et al.*, "Handbook of X-Ray Photoelectron Spectroscopy," Perkin Elmer (Physical Electronics Division), Eden Prairie, 1978.
28. Dickinson, T., Povey, A. F., and Sherwood, P. M. A., *J. Chem. Soc. Faraday Trans. I* **72**, 686 (1976).
29. Barbaray, B., Contour, J. P., and Mouvier, G., *Env. Sci. Technol.* **12**, 1294 (1978).
30. Pretsch, E., Seibl, J., Simon, W., and Clerc, P. D., "Strukturaufklärung organischer Verbindungen mit spektroskopischen Methoden," Springer-Verlag, Berlin, 1981.
31. Himmelblau, D. M., "Process Analysis by Statistical Methods," Wiley, New York, 1970.
32. Efstathiou, A. M., and Fliatoura, K., *Appl. Catal. B: Environmental* **6**, 35 (1995).
33. Schneider, H., Scharf, U., Wokaun, A., and Baiker, A., *J. Catal.* **147**, 545 (1994).
34. Odriozola, J. A., Heinemann, H., Somorjai, G. A., la Banda, J. F. G. d., and Pereira, P., *J. Catal.* **119**, 71 (1989).
35. Srnak, T. Z., Dumesic, J. A., Clausen, B. S., and E., *J. Catal.* **135**, 246 (1992).
36. Kugler, E. L., Kadet, A. B., and Gryder, J. W., *J. Catal.* **41**, 72 (1976).
37. Schraml-Marth, M., Wokaun, A., Curry-Hyde, H. E., and Baiker, A., *J. Catal.* **134**, 75 (1992).
38. Janssen, F. J. J. G., den Kerkhof, F. M. G. v., Bosch, H., and Ross, J. R. H., *J. Phys. Chem.* **91**, 5921 (1987).
39. Kittrell, J. R., Eldridge, J. W., and Conner, W. C., *Catalysis* **9**, 126 (1992).
40. Zhang, G., Buckingham, S., Curry-Hyde, H. E., and Cant, N., *APCChE* **3**, 31 (1993).